BJR

Received: 28 June 2015 | Revised: 28 September 2015 | Accepted: 5 October 2015

doi: 10.1259/bjr.20150528

Cite this article as:
Lynskey SJ, Pianta MJ. MRI and thallium features of pigmented villonodular synovitis and giant cell tumours of tendon sheaths: a retrospective single centre study of imaging and literature review. *Br J Radiol* 2015; **88**: 20150528.

FULL PAPER

MRI and thallium features of pigmented villonodular synovitis and giant cell tumours of tendon sheaths: a retrospective single centre study of imaging and literature review

SAMUEL J LYNSKEY, MB BS and MARCUS J PIANTA, FRANZCR

Radiology Department, St Vincent's Hospital, Melbourne, VIC, Australia

Address correspondence to: Dr Samuel J Lynskey
E-mail: *samlynskey@gmail.com*

Objective: The purpose of this study was to characterize the MRI and thallium-201 (^{201}TI) scintigraphy attributes of pigmented villonodular synovitis (PVNS) and giant cell tumours of tendon sheaths (GCTTS). The epidemiology of these uncommon lesions was also assessed and less commonly encountered pathology reported on including multifocality, necrosis and concurrent malignancy.
Methods: A retrospective single centre review of MRI and ^{201}TI scintigraphy findings for 83 surgically proven or biopsy-proven consecutive cases of PVNS was undertaken. Radiological findings including lesion size, ^{201}TI uptake (as a marker of metabolic activity), location, extent and patient demographics were correlated with biopsy and surgical specimen histology. Typical appearances are described, as well as less common imaging manifestations. The study period encompassed all patients presenting or referred to a tertiary bone and soft-tissue tumour referral centre with PVNS or GCTTS between 1 January 2007 and the 1 December 2013.
Results: Lesions occur most commonly around the knee joint in the fourth decade of life, with younger patients showing a tendency to occur in the hip. Features of PVNS and GTTS include bone erosion, ligamentous and cartilage replacement, muscle infiltration and multifocality. MR signal characteristics were variable but post-contrast enhancement was near-universal. 14 of 83 cases showed no uptake of ^{201}TI and revealed a statistically significant smaller average axial dimension of 19.8 mm than lesions displaying active ^{201}TI uptake of 36.4 mm, $p = 0.016$. Four lesions demonstrated central necrosis on gross histology, two of each from both the ^{201}TI-avid and ^{201}TI-non-avid groups.
Conclusion: MR is the imaging modality of choice when considering the diagnosis of these uncommon tumours. ^{201}TI scintigraphy as a marker of metabolic activity further adds minimal value although small lesions can appear to lack ^{201}TI avidity.
Advances in knowledge: This article depicts typical imaging findings of PVNS/GCTTS and also a subset of lesions that demonstrate no uptake on metabolic functional imaging, namely smaller sized lesions irrespective of anatomical location. This represents an important departure from previously documented imaging manifestations, whereby an absence of isotope accumulation suggested exclusion of these lesions from the differential diagnosis. These findings have important implications when considering the diagnosis of these uncommon lesions and may be important when interpreting post-treatment response. We suggest that further investigation, for example, with MRI is valuable in order to clarify potential post-treatment response, as well as the use of alternate functional imaging modalities such as positron emission tomography (PET), to further corroborate these findings.

INTRODUCTION

Classically functional imaging such as thallium-201 (^{201}TI) scintigraphy has been advocated to assist the differentiation between malignant and benign soft-tissue neoplasms.[1] Increased isotope accumulation (Figures 1 and 2) has been demonstrated for both pigmented villonodular synovitis (PVNS) and giant cell tumours of tendon sheaths (GCTTS) in both early and delayed phase imaging, which may mimic malignant disease.[1–3] Recurrent PVNS and GCTTS demonstrate similar ^{201}TI uptake patterns on early and delayed phase sequences.[4] It has been reported that lesions with low isotope accumulation, suggesting low metabolic activity, are highly unlikely to be PVNS or GCTTS.[1] Despite this, ^{201}TI accumulation has been shown to be dependant on the blood flow in the early "static scan" and isotope accumulation to correlate with the size of the tumour,

Figure 1. 40-year-old female with extensive pigmented villonodular synovitis (PVNS; surgical resection histology) of the right hip. Coronal T_1 weighted (a) and axial short tau inversion–recovery (b) MRI sequences reveal severe erosive disease because of the soft-tissue mass (PVNS). Axial imaging reveals the extent of the femoral and acetabular erosion (arrow) and surrounding soft-tissue infiltration. Thallium-201 (^{201}TI) scintigraphy (c) shows retention at 4 h and angiography (d) shows prominent vascularity of the tumour.

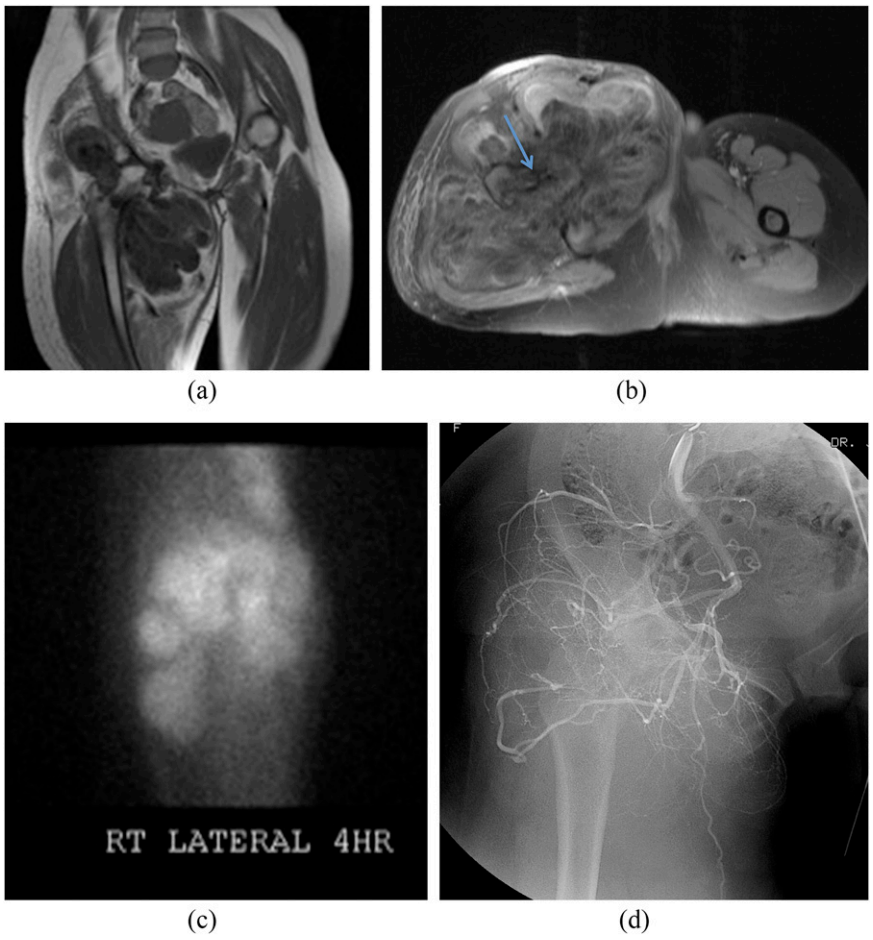

suggesting that smaller and less vascular lesions may not be as well visualized with ^{201}TI scintigraphy (Figure 3).[5] Vascularity, even in small lesions, can be well demonstrated with colour Doppler ultrasound (Figure 4).

Although plain radiography is often performed early in the investigation of a lesion or pain that can be subsequently attributed to PVNS/GCTTS, MRI is the preferred imaging modality for lesion characterization and anatomical definition. On both T_1 and T_2 weighted MRI sequences, PVNS displays heterogeneous low-signal intensity relative to normal skeletal muscle, owing to the high haemosiderin content in xanthoma cells, rich collagen proliferation and a reduction in the T_2 relaxation time.[6,7] Lesions may occasionally be isointense or slightly hyperintense to muscle on T_1 weighted images secondary to the presence of lipid-laden macrophages or haemorrhage.[8] Such hyperintensity as seen on T_1 weighted sequences is regarded as an uncommon finding.[6] Generally, GCTTS will appear as *predominantly* low-signal intensity on both T_1 and T_2 weighted sequences.[9,10] On T_2 weighted sequences, these lesions may appear homogeneous and of equivalent signal intensity to that of the skeletal muscle whilst occasionally appearing inhomogeneous and slightly hyperintense.[9] A peripheral rim of low-signal intensity (capsule) may be seen owing to haemosiderin deposition within the synovium or fibrosis.[8] For both PVNS and GCTTS, strong enhancement is often seen with gadolinium-diethylenetriamine penta-acetic acid–enhanced T_1 weighted images.[7] "Blooming artefact" (Figure 5) results from the magnetic susceptibility of haemosiderin and is seen on T_2* weighted gradient-echo sequences, a phenomenon not as appreciable in differential lesions such as synovial chondromatosis.[7] This effect tends to be blunted with fat-suppressed images and may not be present in immature lesions.[11] A joint effusion is commonly seen in diffuse disease and bony lesions/erosions (Figures 1, 6 and 7) appreciated most commonly in the hip, ankle, elbow and wrist.[11]

For nodular and diffuse forms of PVNS, signal characteristics are reported not to differ appreciably.[12] At our institution, MRI the preferred imaging modality for visualizing these lesions both to exclude alternate pathology and plan biopsy and surgery.

Whilst ^{201}TI uptake in a diffuse nodular juxta-articular pattern (Figure 2) is highly suggestive of PVNS,[2] there is minimal

Figure 2. 46-year-old male with pigmented villonodular synovitis of the knee (surgically and biopsy proven). Thallium-201 (^{201}TI) scintigraphy at 4 h reveals isotope uptake about the knee joint in a juxta-aticular or synovial distribution.

literature available on nuclear medicine, including ^{201}TI, features of PVNS when considering lesion size, anatomical distribution, age and sex characteristics. This study aims to clarify the pattern of ^{201}TI uptake, as a surrogate for a metabolically active lesion, to determine whether lesion uptake is related to tumour size; and to compare the literature-reported MRI findings with those found in this study cohort using both experienced and non-experienced observers. Less commonly encountered histological and imaging findings for PVNS and GCTTS are also described.

Figure 3. 50-year-old female with biopsy-proven pigmented villonodular synovitis of the right knee, which revealed necrosis on histological examination. A focal lesion (a) is noted posterior to the posterior cruciate ligament, which is mildly hyperintense on axial fluid-sensitive sequencing (arrow). Notably, minimal thallium uptake is demonstrated in the right knee on delayed imaging (b).

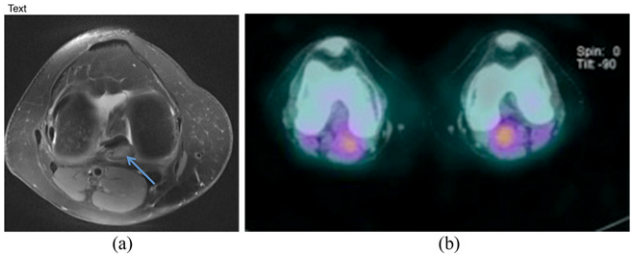

(a) (b)

Figure 4. 30-year-old female, colour Doppler ultrasound (transverse) demonstrates a left ring finger giant cell tumour of tendon sheaths with increased vascularity.

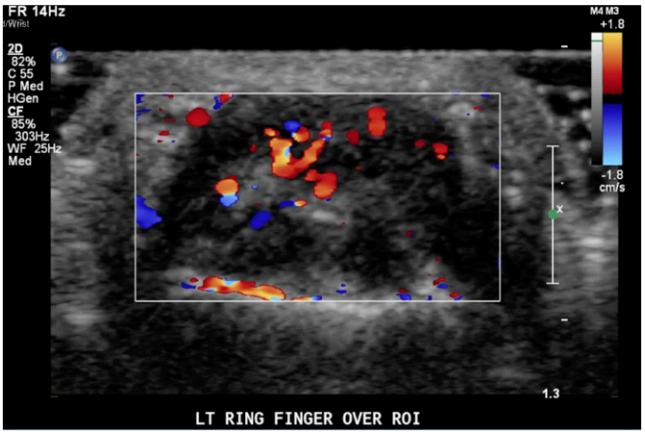

METHODS AND MATERIALS

Approval for the study was gained *via* institutional research ethics review committee. The study period encompassed all patients, 139 in total, who presented to a tertiary orthopaedic tumour referral centre, with a surgically proven or biopsy-proven histological diagnosis of PVNS or GCTTS between the first of January 2007 and the first of December 2013. A retrospective single-centre review of imaging findings was undertaken. Localized radiological appearances including lesion size, location, extent, MRI and ^{201}TI scintigraphy (both studies performed as a part of the referring orthopaedic tumour unit workup) attributes were correlated with subject demographics as well as biopsy and surgical specimen histology. Typical and less common imaging manifestations were noted. Lesion measurements and extent of ^{201}TI uptake were reviewed and compared with the contralateral side for both early (30 min) and delayed phase (4 h) single-photon emission CT (SPECT) sequences, after the injection of 148 MBq (4 mCi) of ^{201}TI. These were performed predominantly on Siemens Symbia T6 and T16 γ cameras (Siemens, Hoffman Estates, IL) with low-energy, high-resolution collimation on a 128×128 matrix. MRI machines included a Siemens 1.5-T Avanto and 1.5-T Symphony (Siemens Healthcare Systems, Erlangen, Germany) and signal characteristics were described as demonstrating diffuse enhancement, peripheral enhancement or no enhancement for post-gadolinium T_1 contrast studies and signal intensity for T_1 and T_2 weighted MRI sequences described as hyper-, hypo- or iso-intense to that of the surrounding muscle. Two independent reviewers, one musculoskeletal radiologist and one resident measured lesions in the greatest axial diameter from the pre-biopsy ^{201}TI scan SPECT, which was available for 83 of the 139 subjects studied. Discrepancies were resolved by consensus for MRI signal characteristics, and lesion size measurements were averaged if they differed by $<10\%$ and resolved by consensus if they differed by $>10\%$. Lesions were classified as focal if localized to one area of the synovium or as diffuse if most or all of the synovium was involved when visualized using MRI. Statistical analysis was performed using Microsoft® Excel® (Microsoft, Redmond, WA), and standard deviations were calculated for the

Figure 5. 53-year-old female with surgically proven pigmented villonodular synovitis of the right knee commencing above the level of the knee and extending into the calf with the neurovascular bundle effaced posterolaterally. Blooming artefact (arrow) is demonstrated on axial gradient-echo sequencing (a). Post-contrast T_1 fat-saturation sagittal sequence shows marked synovial thickening and an enhancing mass within the popliteal fossa (b).

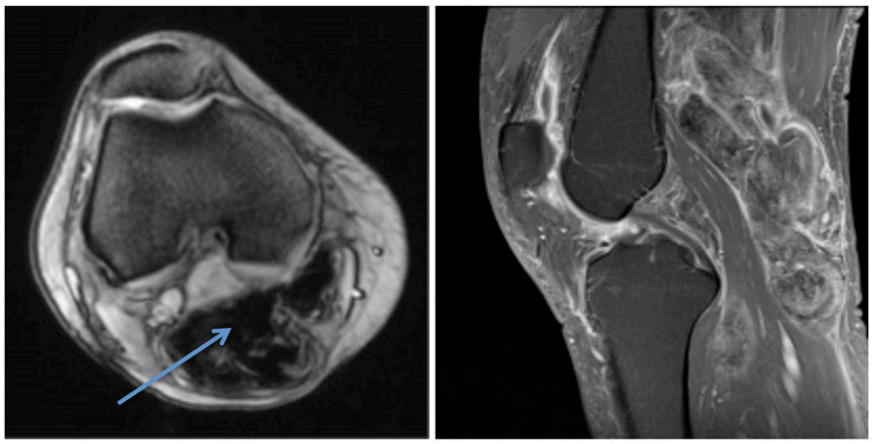

^{201}TI-avid and ^{201}TI-non-avid sample groups. Interobserver agreement was calculated using Cohen's κ equation and *p*-values calculated using two-tailed, independent *t*-tests. Ages were calculated at the time of biopsy or at the time of surgery if biopsy was not available.

RESULTS

In terms of anatomical distribution of PVNS/GCTTS, in our study cohort lesions predominantly occurred in the knee 55.4% of the time, followed by the ankle, hip, toe, finger, foot, and wrist (Table 1). PVNS affected females in 51% of the cases and males in 49%. 62 lesions (45%) were identified as diffuse and 77 (55%) as focal. Lesions identified as GCTTS comprised 8.6% of all lesions and affected males and females equally. GCTTS was found to occur most commonly in the extremities with the toe being the most common site of occurrence (3.6%), followed by the finger (2.2%), foot, ankle and hand (0.7%). Lesions affecting the digits and wrist made up 10.8% of all lesions. Less common sites of occurrence included in the "other" category (Table 1) comprised the calf, elbow and pes anserinus, with only 2.1% of all lesions.

When considering age at the time of biopsy, the most common site of occurrence was the knee joint (55.4%) (Figures 2, 3 and 5) in the fourth decade of life (Table 2). The second most common site of occurrence for all age groups was the ankle joint (20.9%), except in the under-20 age group where the hip joint was the second most commonly involved (20%) compared with the ankle joint (10%). In the 20- to 29-year-old age group, the hip was the third most common site of occurrence, whereas in the remaining age groups, the third most common sites affected were the extremities, primarily the digits and feet.

Figure 6. 30-year-old female with surgically proven pigmented villonodular synovitis of the right ankle. MRI T_1-post-contrast fat saturation (a) and sagittal short tau inversion–recovery (b) sequences reveal marked swelling around the ankle joint, a well-defined anterior and posterior soft-tissue lesion, which extends into the syndesmosis and involves the anterior and posterior inferior tibiofibular ligaments, and extends into the flexor tendon sheaths. Associated bony erosion is also noted.

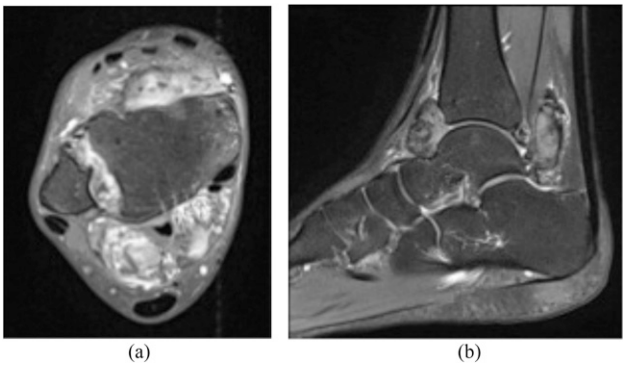

Figure 7. 55-year-old female with biopsy proven giant cell tumours of tendon sheaths of the left first metatarsophalangeal joint. T_1 weighted MRI reveals a hypointense soft-tissue mass extending deep to the subdermis with severe bony erosion, ligamentous and tendon involvement.

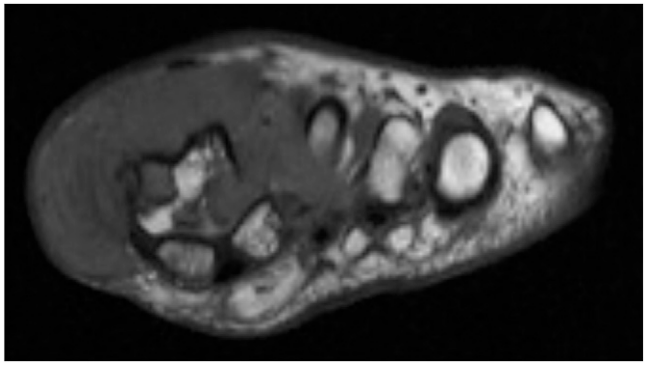

Table 1. Gender and average age per disease location

Location	Number of lesions at site	% of lesions at site	Male	Female	Male : female	Average age (years)
Ankle	29	20.9	17	12	1.4 : 1	40
Foot	6	4.3	1	5	1 : 5	42
Hip	9	6.5	3	6	1 : 2	32
Knee	77	55.4	37	40	1 : 1	39
Wrist/phalanges	15	10.8	6	9	1 : 1.5	43
Other	3	2.1	3	0	3 : 0	50
Total	139	100	67	72		

Lesions comprising the "other" category include calf, elbow, and pes anserinus.

Post-gadolinium contrast studies were most consistently agreed upon in this study, with excellent correlation ($K = 0.97$) (Table 3). T_2 signal was described with moderately high correlation ($K = 0.54$). T_1 weighted signal sequences were the most difficult to agree upon, with a lower level of, albeit still moderate, correlation ($K = 0.45$).

T_1, T_2 and post-contrast imaging was available for a total of 123 cases. Lesions predominantly revealed T_1 and T_2 hypointense signal 54% and 79% of the time, respectively, and 99% demonstrated post-gadolinium contrast enhancement. Lesions were hyperintense 35% of the time on T_1 weighted imaging *vs* 20% on T_2 weighted imaging. Post-contrast studies revealed gadolinium contrast uptake almost universally, with only 1% of all lesions demonstrating no appreciable enhancement. Of lesions demonstrating enhancement post contrast, 99% of these revealed diffuse enhancement, whereas 1% enhanced in the periphery of the lesion only.

^{201}TI-avid lesions (83% of the sample population) exhibited a maximal axial diameter mean of 36.4 mm and a range from 12.3 to 185 mm. ^{201}TI-non-avid lesions (17% of the sample population) exhibited a maximal axial diameter mean of 19.8 mm and a range from 6.8 to 45 mm and were statistically smaller than the ^{201}TI-avid group with a p-value of 0.016 from a two-sided t-test. Of ^{201}TI-avid lesions, early and delayed phase radiotracer uptake was universal. Of ^{201}TI-non-avid lesions, 86% demonstrated no uptake on both early and delayed phase sequences. The remaining 14% demonstrated early uptake only. A similar anatomical distribution was seen in the ^{201}TI-avid group as in the entire study population. The ^{201}TI-non-avid group also demonstrated the knee as the most common location but was slightly atypical with the hip being the second most common location for lesions—a site noted to be more commonly involved in the younger population (Table 4).

Table 2. Anatomical lesion location according to age

Age (years)	Total number of lesions (139)	Most common site (%)	Second most common site (%)
<20	10	Knee (60)	Hip (20)
20–29	28	Knee (64)	Ankle (21)
30–39	42	Knee (52)	Ankle (24)
40–49	23	Knee (52)	Ankle (17)
50–59	20	Knee (50)	Ankle (25)
60–69	12	Knee (58)	Ankle (17)
>70	4	Knee (50)	Ankle (25)

No statistically significant difference was found between the ^{201}TI-avid and ^{201}TI-non-avid groups when considering age at the time of biopsy with a p-value of 0.35.

In the ^{201}TI-non-avid group, two lesions displayed necrosis on gross histological examination (14% of the sample). Both cases were located at the knee joint and correlated with a history of recent patient trauma (specifically hyperextension injuries). In the ^{201}TI-avid group, two lesions demonstrated infarction on histological examination (comprising just 3% of the sample), one occurring intra-articularly in the hip joint and the other in the knee. Both these lesions demonstrated hyperintense signal on T_1 and T_2 weighted MRI sequences. Contrast MRI studies were not performed for either of the necrotic or infarcted lesions.

Of interest, PVNS was found to occur concurrently with chondrosarcoma on histological examination in a single patient.

DISCUSSION

Our findings support the current epidemiological distribution of these lesions.[13]

The classic description of PVNS supports heterogeneous low to isointense signal on both T_1 and T_2 weighted sequences, although variable, and is generally determined by cellular architecture. We also demonstrated predominantly hypointense T_1 and T_2 signal (when compared with surrounding normal muscle), with good interobserver correlation between

Table 3. Lesion appearance based on signal weighting and level of agreement between experienced and non-experienced observers for all lesions visualized using MRI

MRI sequence	Hypointense		Hyperintense		Isointense		Total number of lesions (%)	Kappa	Level of agreement
	Number of lesions (%)	% agreement	Number of lesions (%)	% agreement	Number of lesions (%)	% agreement			
T_1 weighted sequences	67 (54)	72	43 (35)	20	13 (11)	7	123 (100)	0.45	Low and moderate
T_2 weighted sequences	97 (79)	96	25 (20)	60	1 (1)	0.9	123 (100)	0.54	High and moderate
Post-contrast sequences	1 (1)	0	86 (99)	98	0	0	87 (100)	0.97	Very good

experienced and non-experienced observers. However, a significant number of lesions did display hyperintense signal on T_2 weighted sequences, and up to one-third of cases displayed hyperintensity on T_1 weighted sequences. Diffuse post-contrast enhancement was almost universally demonstrated. T_2 and post-contrast sequencing were most consistently reported amongst the two observers, with T_1 signal showing the most variability, possibly due to the degree of hypo- or hyperintensity being marginal or less appreciable than on T_2 weighted sequences. MRI signal characteristics for PVNS and GCTTS do not differ based on anatomical location or distribution.

Lesion size was measured pre-biopsy using ^{201}TI SPECT axial images, where each reviewer measured the greatest axial dimension, and the values averaged for a single measurement (>10% discrepancy was addressed by consensus). We acknowledge that whilst this is a low-dose and lower spatial resolution scan than a diagnostic CT scan or MRI, it was available with axial images and for all patients, lending to consistency and comparable measurements. One possible explanation for the significantly smaller lesion size in the ^{201}TI-non-avid group (19.8 *vs* 36.4 mm, $p = 0.008$) may relate to an inability of SPECT to resolve uptake in smaller lesions. This may also partly be attributable to reduced blood flow in smaller lesions, thus precluding an adequate amount of isotope necessary for sequestration before ^{201}TI avidity can be visualized. In a study by Sato et al[5] who evaluated a series of benign and malignant tumours of the head and neck; ^{201}TI accumulation was shown to be dependant on the blood flow in the early "static scan" and isotope accumulation correlated with the size of the tumour.

^{201}TI-positive lesion distribution was representative of the whole population, whereas ^{201}TI-non-avid lesions showed a greater tendency to occur at the hip. Two lesions did not demonstrate ^{201}TI avidity but displayed necrosis on gross histological examination that further suggests the importance of blood flow to visualization using ^{201}TI SPECT. It should be noted that necrosis is regarded as a rare finding in the literature—two cases each of which we demonstrated in both ^{201}TI-non-avid and ^{201}TI-positive groups.[14]

Given a lack of correlation with necrosis, negative uptake in smaller lesions and inferior spatial resolution, this series demonstrates that ^{201}TI scintigraphy has a very limited role in evaluating PVNS/GCTTS. MRI remains the preferred imaging modality at St Vincent's Hospital, Melbourne, VIC, given its characteristic and consistent appearances and superior spatial resolution. With rare potential for malignant transformation, however (and concurrence with chondrosarcoma in a single case in this study), we cannot advocate for the use of tissue sampling to establish the diagnosis of PVNS/GCTTS unless dictated clinically in accordance with the treating unit.

CONCLUSION

Lesions occur most commonly around the knee joint in the fourth decade of life, with younger patients showing a tendency to occur

Table 4. Thallium (^{201}TI)-positive *vs* ^{201}TI-non-avid lesions with respect to lesion size, location, atypical features and age at the time of biopsy

^{201}TI avidity	Number of lesions	Average maximal axial size (mm)	Most common location (cases, % total)	Second most common location (cases, % total)	Necrosis cases (% total)	Average age at the time of biopsy (years)
^{201}TI positive	69	36.4	Knee (39, 56%)	Ankle (17, 25%)	2 (3%)	40
^{201}TI negative	14	19.8	Knee (7, 50%)	Hip (4, 29%)	2 (14%)	43

in the hip. MR is the imaging modality of choice demonstrating generally lower T_1 and T_2 signal with post-contrast enhancement and for which interobserver interpretation is very reliable between experienced and non-experienced observers. ^{201}TI scintigraphy offers minimal additional value, and smaller lesions are more likely to be non-avid.

ACKNOWLEDGMENTS

The authors thank Stephen Schlicht, John Slavin and Peter Choong for academic discourse and access to research material and facilities. Portions of this study have been presented in abstract form at the 10th Asia Pacific Musculoskeletal Tumour Society (APMSTS) Meeting, Melbourne, VIC, Australia, Friday 11 April 2014.

REFERENCES

1. Kawakami N, Kunisada T, Sato S, Morimoto Y, Tanaka M, Sasaki T, et al. Thallium-201 scintigraphy is an effective diagnostic modality to distinguish malignant from benign soft-tissue tumors. *Clin Nucl Med* 2011; **36**: 982–6. doi: 10.1097/RLU.0b013e3182177407
2. Koto K, Murata H, Sakabe T, Matsui T, Horie N, Sawai Y, et al. Magnetic resonance imaging and thallium-201 scintigraphy for the diagnosis of localized pigmented villonodular synovitis arising from the elbow: a case report and review of the literature. *Exp Ther Med* 2013; **5**: 1277–80.
3. Mackie GC. Pigmented villonodular synovitis and giant cell tumor of the tendon sheath: scintigraphic findings in 10 cases. *Clin Nucl Med* 2003; **28**: 881–5. doi: 10.1097/01.rlu.0000093083.77866.5c
4. Kobayashi H, Sakahara H, Hosono M, Shirato M, Konishi J, Kotoura Y, et al. Scintigraphic evaluation of tenosynovial giant-cell tumor using technetium-99m(V)-dimercaptosuccinic acid. *J Nucl Med* 1993; **34**: 1745–7.
5. Sato T, Kawabata Y, Kobayashi Y, Suenaga S, Indo H, Kawano K, et al. Scintigraphy for interpretation of malignant tumours of the head and neck: comparison of technetium-99m-hexakis-2-methoxyisobutylisonitrile (Tc-MIBI) and thallium-201-chloride (Tl-201). *Dentomaxillofac Radiol* 2005; **34**: 268–73. doi: 10.1259/dmfr/65143191
6. Murphey MD, Rhee JH, Lewis RB, Fanburg-Smith JC, Flemming DJ, Walker EA. Pigmented villonodular synovitis: radiologic-pathologic correlation. *Radiographics*. 2008; **28**: 1493–518. doi: 10.1148/rg.285085134
7. Papp DF, Khanna AJ, McCarthy EF, Carrino JA, Farber AJ, Frassica FJ. Magnetic resonance imaging of soft-tissue tumours: determinate and indeterminate lesions. *J Bone Joint Surg Am* 2007; **89**(Suppl. 3): 103–15. doi: 10.2106/JBJS.G.00711
8. Al-Nakshabandi NA, Ryan AG, Choudur H, Torreggiani W, Nicoloau S, Munk PL, et al. Pigmented villonodular synovitis. *Clin Radiol* 2004; **59**: 414–20. doi: 10.1016/j.crad.2003.11.013
9. De Beuckeleer L, De Schepper A, De Belder F, Goethem JV, Marques MC, Broeckx J, et al. Magnetic resonance imaging of localized giant cell tumour of the tendon sheath (MRI of localized GCTTS). *Eur Radiol* 1997; **7**: 198–201. doi: 10.1007/s003300050134
10. Jelinek JS, Kransdorf MJ, Shmookler BM, Aboulafia AA, Malawer MM. Giant cell tumor of the tendon sheath: MR findings in nine cases. *AJR Am J Roentgenol* 1994; **162**: 919–22. doi: 10.2214/ajr.162.4.8141018
11. Cheng XG, You YH, Liu W, Zhao T, Qu H. MRI features of pigmented villonodular synovitis (PVNS). *Clin Rheumatol* 2004; **23**: 31–4. doi: 10.1007/s10067-003-0827-x
12. Poletti S, Gates 3rd H, Martinez S, Richardson W. The use of magnetic resonance imaging in the diagnosis of pigmented villonodular synovitis. *Orthopedics* 1990; **13**: 185–90.
13. Bruns J, Ewerbeck V, Dominkus M, Windhager R, Hassenpflug J, Windhagen H, et al. Pigmented villo-nodular synovitis and giant-cell tumor of tendon sheaths: a binational retrospective study. *Arch Orthop Trauma Surg* 2013; **133**: 1047–53. doi: 10.1007/s00402-013-1770-1
14. O'Connell JX. Pathology of the synovium. *Am J Clin Pathol* 2000; **114**: 773–84.